Multi-GeV Energy Gain in a Plasma-Wakefield Accelerator

M. J. Hogan,[1] C. D. Barnes,[1] C. E. Clayton,[2] F. J. Decker,[1] S. Deng,[3] P. Emma,[1] C. Huang,[2] R. H. Iverson,[1] D. K. Johnson,[2] C. Joshi,[2] T. Katsouleas,[3] P. Krejcik,[1] W. Lu,[2] K. A. Marsh,[2] W. B. Mori,[2] P. Muggli,[3] C. L. O'Connell,[1] E. Oz,[3] R. H. Siemann,[1] and D. Walz[1]

[1]*Stanford Linear Accelerator Center, Stanford University, Stanford, California 94309, USA*
[2]*University of California, Los Angeles, California 90095, USA*
[3]*University of Southern California, Los Angeles, California 90089, USA*

(Received 25 March 2005; published 28 July 2005)

A plasma-wakefield accelerator has accelerated particles by over 2.7 GeV in a 10 cm long plasma module. A 28.5 GeV electron beam with 1.8×10^{10} electrons is compressed to 20 μm longitudinally and focused to a transverse spot size of 10 μm at the entrance of a 10 cm long column of lithium vapor with density 2.8×10^{17} atoms/cm^3. The electron bunch fully ionizes the lithium vapor to create a plasma and then expels the plasma electrons. These electrons return one-half plasma period later driving a large amplitude plasma wake that in turn accelerates particles in the back of the bunch by more than 2.7 GeV.

DOI: 10.1103/PhysRevLett.95.054802 PACS numbers: 41.75.Ht, 41.75.Lx, 52.25.Jm, 52.40.Mj

Plasmas have extraordinary potential for advancing the energy frontier in high-energy physics due to the large focusing and accelerating fields that are generated. Beam-plasma interactions have demonstrated focusing gradients of MT/m [1] while laser plasma interactions have demonstrated GeV/cm accelerating gradients [2–7] over distances of a few mm. Beam-driven plasma-wakefield accelerators (PWFA) have recently demonstrated acceleration and focusing of both electrons [8,9] and positrons [10,11] in meter scale plasmas.

The experiment described in this Letter uses an ultrarelativistic electron bunch to simultaneously create a plasma in lithium vapor and drive a large amplitude plasma wave. When the electron bunch enters the lithium vapor, the electric field of the leading portion of the bunch ionizes the valence electron of each lithium atom in its vicinity leaving fully ionized neutral plasma for the remainder of the bunch [12,13]. The plasma electrons are then expelled from the beam volume and return one-half plasma period later. The returning plasma electrons form density concentrations on axis behind the bunch leading to a large accelerating field for the particles in the back of the bunch.

In linear plasma theory [14] the wakefield amplitude increases as $\sim N/\sigma_z^2$, provided the plasma density is increased such that $k_p\sigma_z \approx \sqrt{2}$ where N is the number of electrons in the bunch, σ_z is the bunch length, and $k_p = \omega_p/c$ is the inverse of the plasma collisionless skin depth. The nonlinear or blowout regime is reached when the electron bunch density $n_b = N/[(2\pi)^{3/2}\sigma_z\sigma_r^2]$ is greater than the plasma density n_p and the beam radius satisfies $\sigma_r \ll c/\omega_p$. In the blowout regime, for bunch lengths on the order of the plasma wavelength, the plasma electrons are expelled from the beam volume to a radius $r_c = 2\sqrt{N/[(2\pi)^{3/2}\sigma_z n_p]}$ leaving behind a pure ion column. This experiment is in a regime in which the electron bunch radius, bunch length, ion channel radius, and plasma wavelength are all on the same order. Although the experiments described here are on the edge of the blowout regime, numerical simulations indicate the N/σ_z^2 increase in plasma-wakefield amplitude can still be realized [15]. Verification of the dramatic increase in accelerating gradient predicted for short bunches is a critical milestone for the application of plasma-wakefield accelerators to future high-energy accelerators and colliders.

A single 28.5 GeV bunch of 1.8×10^{10} electrons from the Stanford Linear Accelerator Center (SLAC) linac enters the Final Focus Test Beam (FFTB) beam line at a rate of 1 or 10 Hz. Bunch position and charge are measured with beam position monitors and toroidal current monitors. The Optical Transition Radiation (OTR) produced as the bunch passes through 1 μm thick titanium (Ti) foils is imaged onto cooled charge coupled device (CCD) cameras to measure the transverse profile of the bunch before and after the plasma. The OTR before the plasma is used for tuning the incoming beam and the OTR after the plasma provides information about plasma focusing and deflection [8,9,16,17]. At wavelengths longer than the bunch length the transition radiation becomes coherent (CTR), and the integrated CTR energy increases as the bunch length becomes shorter. The CTR energy radiated from another 1 μm Ti foil before the plasma is measured with a pyroelectric detector and used to monitor the relative bunch length on a shot-to-shot basis. The energy lost to longitudinal wakefields in the linac also increases as the bunch length becomes shorter and correlates well with the total CTR energy recorded by the pyroelectric detector. Autocorrelation of the average bunch profile with a CTR based Michelson interferometer confirms the fully compressed bunches are on the order of 12 μm (rms). Dipole magnets after the plasma vertically disperse the bunch in energy while quadrupole magnets image the bunch exiting the plasma onto a 1 mm thick piece of fused silica aerogel. This imaging energy spectrometer is crucial for differentiating plasma induced energy changes to the beam from

possible transverse deflections caused by the strong focusing forces of the ion channel. The Cherenkov light emitted by the beam passing through the aerogel is imaged onto a cooled CCD camera. The vertical projection of the resulting image is the energy spectrum of the bunch exiting the plasma.

Previous experiments [8,10] used a streak camera to time resolve the energy spectrum resulting from the plasma. There are no techniques available to time resolve the spectrum of 12 μm (40 fs) bunches; consequently, the energy changes from the plasma are measured by comparing the time integrated energy spectrum of the bunch with and without the plasma. The energy spectrum before the plasma is measured with a noninvasive spectrometer similar in design to devices described by Seeman *et al.* [18]. In a region where the energy spread dominates the beam size, a two-meter long chicane gives a slight vertical deflection to the electron bunch. The intensity of the resulting stripe of synchrotron radiation is a measure of the transverse projection and thus the energy spectrum. The x-ray portion of the synchrotron spectrum scintillates in a cerium doped yttrium aluminum garnet (Ce:YAG) screen which is imaged onto a cooled CCD camera. All diagnostics are recorded on a shot-to-shot basis.

The lithium vapor is created in a heat pipe oven [19] where the neutral lithium vapor density and length are controlled through the temperature of the oven and the pressure of the helium buffer gas which confines the hot lithium at both ends. Lithium has a relatively low ionization potential for the first electron (5.4 eV) that allows ionization sufficient for wakefield generation for a broad range of beam parameters. The larger ionization potential of the second electron (75.6 eV) ensures the plasma density does not evolve significantly along the bunch due to secondary ionization. Previous experiments [8–11,16,17] ionized the lithium vapor with an excimer laser operating at 193 nm and controlled the plasma density with the laser energy [19]. In the experiments described here, the neutral lithium vapor is fully ionized by the large radial electric field of the compressed electron bunches [12,13] and the plasma density is then equal to the lithium vapor density. Field-ionized plasma production is advantageous in that there are no timing, lifetime, or alignment issues normally associated with plasmas in this density-length range. The lithium oven can be exchanged with a helium filled bypass line within seconds to compare plasma on and off energy spectra. Field-ionized plasmas offer the possibility to create the many meter long stable plasmas envisioned for future colliders [20,21].

The bunch length was $\sim$700 μm in previous PWFA experiments [8–11,16,17]. In the summer of 2002 a bunch compressor chicane was added at the 9 GeV point roughly one-third of the way down the 3 km SLAC linac. In a three stage process the bunches are now compressed to a predicted minimum of 12 μm rms. The nominal process for maximum compression is as follows [22]. A 6 mm long bunch exits the north damping ring of the accelerator with an energy of 1.19 GeV and is given a correlated energy spread via an rf cavity run at the zero crossing phase such that the mean energy does not change. The resulting correlated energy spread coupled with the nonzero momentum compaction of the ring-to-linac transport line compresses the bunch to 1.2 mm before it reenters the main linac. The phase of the accelerating structures in the linac is set to add an additional energy correlation as the bunch is accelerated to 9 GeV. The magnetic chicane then compresses the bunch to 50 μm. Longitudinal wakefields in the remaining 2 km of linac impose an additional energy correlation which is used to compress the bunch a third and final time to the minimum value of 12 μm in the FFTB. All bunch lengths are rms of Gaussian fits to the measured or inferred distributions. The bunch length and current distribution are adjusted by changing parameters in the main linac as well as the FFTB.

Although there are no diagnostics available to directly measure the current profile of the compressed electron bunches entering the plasma, it is possible to measure it indirectly. Within reasonable ranges of the accelerator parameters that affect the bunch compression process, the energy spectrum measured at the end of the linac is unique. We use the 2D (z, p_z) simulation code LITRACK [23] to match the energy spectra measured in the FFTB with the simulated ones and infer the incoming phase space and current profile. Similar techniques have been used successfully on the Stanford Linear Collider [24] although the bunch length was much longer and fewer factors affected the compression. An example showing a measured single

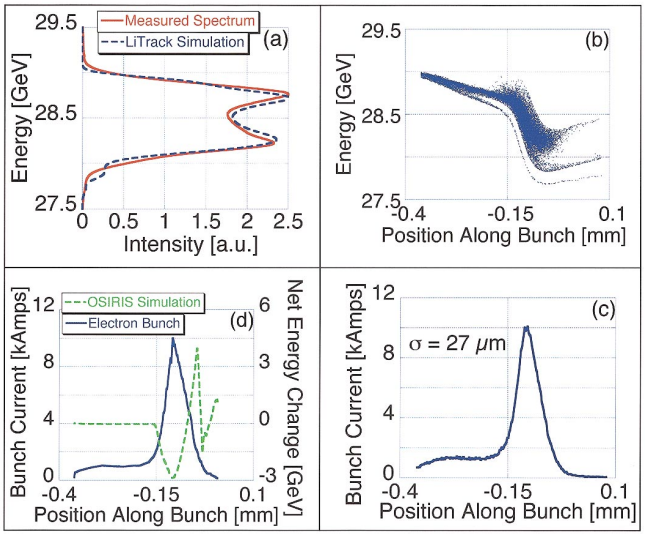

FIG. 1 (color). (a) The measured energy spectrum (solid line) is plotted with the matching spectrum obtained using LITRACK simulations (dashed line). (b) The corresponding simulated longitudinal phase space and (c) reconstructed current profile The current profile indicates that the head of the incoming electron bunch has a long low-current leading edge and a Gaussian shaped high-current core near the back. (d) The current profile from LITRACK (solid line) end the energy change predicted by a 2D OSIRIS simulation (dashed line).

shot energy spectrum, the best match computed using LITRACK, and the reconstituted longitudinal phase space distribution and the current profile are shown in Fig. 1. This example illustrates that the incoming electron bunches have a long low-current leading edge and a Gaussian shaped high-current core. 2D numerical simulations using the code OSIRIS indicate the core of the bunch will lose energy driving the plasma wake while particles in the back of the bunch will gain energy. This predicted energy change is plotted along the bunch current profile in Fig. 1(d). Note that the bunch incoming correlated energy spread is not included in the simulation.

Without the plasma the incoming electron bunch has an energy spread of ~1 GeV FWHM [see Fig. 2(a)]. When the 10 cm long 2.8×10^{17} atoms/cm^3 lithium vapor is inserted, Fig. 2(b) shows the bulk of the electrons lose energy with a maximum loss of 4.1 GeV below the lowest incoming energy. Electrons in the back of the bunch have been accelerated to an energy 2.7 GeV more than the maximum incoming energy. The longitudinal wakefields that give the incoming bunch the correlated energy spread necessary for compression also give the particles in the back of the bunch the lowest energy [see Fig. 1(b)]. Since particles in the back of the bunch sample the largest accelerating field but start from the lowest energy, the highest energy particles measured in Fig. 2(b) have gained on the order of 3.7 GeV in the 10 cm long plasma, i.e., an acceleration gradient of 37 GeV/m. For comparison, the accelerating gradient in the plasma is more than 3 orders of magnitude greater than the gradient in the conventional linac used to produce the incoming bunch. The total number of particles with energy greater than the maximum incoming energy is 7% of the total bunch: 1.25×10^9 electrons—see Fig. 3. The energy spectra after the plasma also show that the energy of the 25% of the electrons contained in the low-current leading edge of the bunch remain unchanged by the addition of the lithium vapor. The electric field along this portion of the bunch is below the threshold necessary to ionize the lithium vapor and thus there is not yet any plasma to transfer energy to.

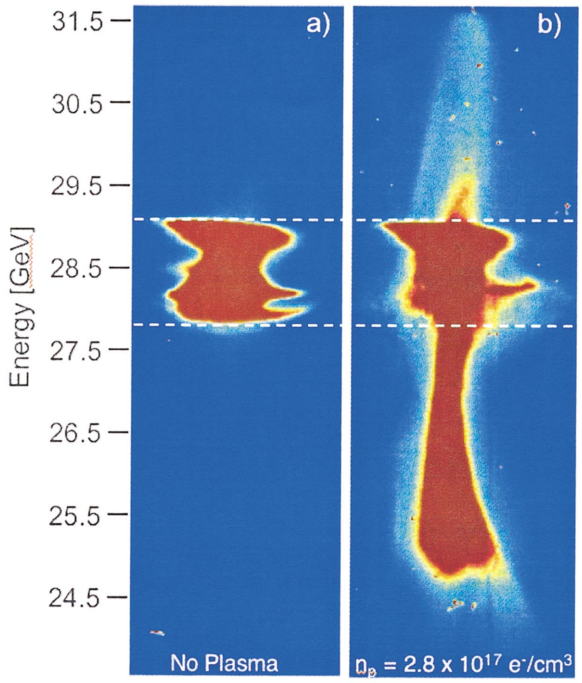

FIG. 2 (color). Single bunch energy spectra downstream from the plasma for (a) the case of no plasma and (b) a 10 cm long 2.8×10^{17} e^-/cm^3 lithium plasma. The no plasma case shows the ~1 GeV energy spread typical of the incoming compressed pulses. At right, the core of the electron bunch has lost energy driving the plasma wake while particles in the back of the bunch have been accelerated to 2.7 GeV over the maximum incoming energy. The images are displayed with a saturated color map to highlight the 7% of the bunch particles accelerated to energies higher than the maximum incoming energy. The peak intensity in both figures is more than a factor of 4 below the saturation level of the camera.

The acceleration signature is repeatable from shot to shot, and for a given vapor or plasma density there is an optimum bunch current profile that produces the maximum energy gain. To quantify the effects of a changing current profile on the wake at fixed vapor or plasma density the following methodology was chosen. A normalized cumulative sum of the bunch charge is performed starting from the highest energy to the lowest energy such that the energy location where the sum is equal to 0.01 would represent the highest energy reached by 1% of the beam. Conversely, the energy value where the sum is 0.99 represents the lowest energy reached by 1% of the beam as illustrated in Fig. 3. This procedure is then performed for a series of consecutive events with variable bunch lengths and acquired at 1 Hz. The energy values are then sorted and binned according to the relative bunch length as given by the integrated CTR energy.

The results for the 1% and 99% contours are plotted for a series of 190 consecutive events with a 10 cm long lithium

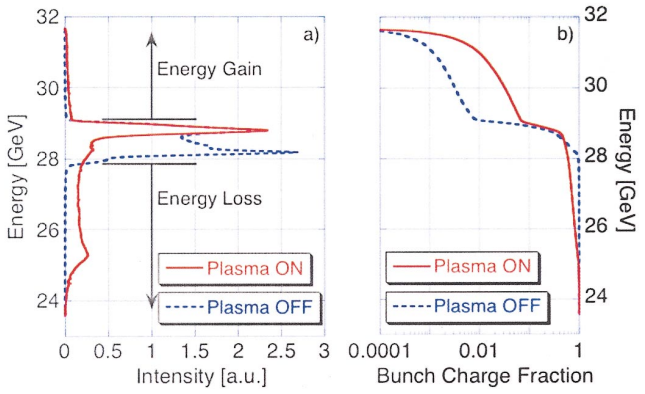

FIG. 3 (color). (a) Energy spectra for a plasma on and off case. 25% of the electrons in the head of the bunch, which also have the highest energies in the plasma off case, are not affected by the lithium vapor. (b) The normalized cumulative charge sum is used to quantify the energy gain or loss of the highest or lowest energy 1% fraction of bunch particles.

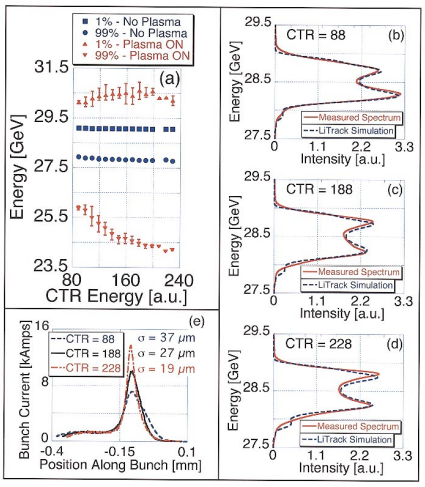

FIG. 4 (color). (a) Binned contours of 1% and 99% of the cumulative normalized bunch charge for plasma on (red) and off (blue) vs the energy signal on the CTR detector. The vertical bars represent the minimum and maximum values for that bin. The measured energy spectrum, matching LITRACK simulation (b)–(d) and corresponding bunch current profiles (e) are shown for three cases: less compressed (37 μm), optimal (27 μm), and further compressed (19 μm), respectively.

vapor density of 2.8×10^{17} atoms/cm^3 in Fig. 4 along with the equivalent contours with no lithium vapor present. The simple nature of the field-ionized plasma source dictates that fluctuations in the measured acceleration will be driven primarily by fluctuations in the incoming electron bunch current profile. Figure 4 shows that for 190 consecutive events where the bunch length and peak current were allowed to fluctuate by over a factor of 2, the acceleration measured by the 1% contour is greater than 1 GeV on every shot. The maximum energy loss measured with the 99% contour increases with shorter bunch lengths (larger CTR energy signal) while the energy gain measured by the 1% contour is maximum at a CTR energy corresponding to a 27 μm long bunch core with a corresponding peak current of 10 kA, as deduced from the LITRACK simulations. When the bunch is less compressed [37 μm and 7 kA, respectively, in Figs. 4(b) and 4(e)] the plasma-wakefield amplitude is lower and thus both the energy gain and loss are consequently lower. When the bunch is further compressed to 19 μm and 14 kA [Figs. 4(d) and 4(e)] the wakefield amplitude is larger, resulting in larger energy loss, but as the bunches become progressively shorter the number of electrons in the region of maximum accelerating field decreases as shown by the 1% contour. It should be emphasized that this optimum is an artifact of the single bunch cases studied here. Future two-bunch plasma accelerators will use one bunch to drive the wake and accelerate a second bunch with narrow energy spread. Provided the intrabunch spacing and plasma density are adjusted accordingly, the measured accelerating gradient in a two-bunch scheme should continue to increase as the drive bunch length is shortened.

In summary, a self-ionized beam-driven plasma-wakefield accelerator has accelerated particles by over 2.7 GeV in a 10 cm long 2.8×10^{17} e^-/cm^3 lithium plasma. This experiment has verified the dramatic increase in accelerating gradient predicted for short drive bunches and has reached several significant milestones for beam-driven plasma-wakefield accelerators: the first to operate in the self-ionized regime, the first to gain more than 1 GeV energy, and the largest accelerating gradient measured to date by 2 orders of magnitude. It is a crucial step in the progression of plasmas from laboratory experiments to future high-energy accelerators and colliders.

The authors would like to thank Dr. Peter Tsou of JPL for the aerogel. This work supported by Department of Energy Contracts No. DE-AC02-76SF00515 (SLAC), No. DE-FG03- 92ER40745, No. DE-FG03-98DP00211, No. DE-FG03-92ER40727, No. DE-AC-0376SF0098, and National Science Foundation Grants No. ECS-9632735, No. DMS-9722121, and No. PHY-0078715.

[1] J. S. T. Ng *et al.*, Phys. Rev. Lett. **87**, 244801 (2001).
[2] D. Gordon *et al.*, Phys. Rev. Lett. **80**, 2133 (1998).
[3] A. Modena *et al.*, Nature (London) **377**, 606 (1995).
[4] V. Malka *et al.*, Science **298**, 1596 (2002).
[5] A. Ting *et al.*, Phys. Rev. Lett. **77**, 5377 (1996).
[6] W. Leemans *et al.*, Phys. Rev. Lett. **89**, 174802 (2002).
[7] D. Umstadter *et al.*, Science **273**, 472 (1996).
[8] P. Muggli *et al.*, Phys. Rev. Lett. **93**, 014802 (2004).
[9] C. E. Clayton *et al.*, Phys. Rev. Lett. **88**, 154801 (2002).
[10] B. Blue *et al.*, Phys. Rev. Lett. **90**, 214801 (2003).
[11] M. J. Hogan *et al.*, Phys. Rev. Lett. **90**, 205002 (2003).
[12] D. L. Bruhwiler *et al.*, Phys. Plasmas **10**, 2022 (2003).
[13] S. Deng *et al.*, Phys. Rev. E **68**, 047401 (2003).
[14] C. Joshi *et al.*, Phys. Plasmas **9**, 1845 (2002).
[15] W. Lu *et al.* (to be published).
[16] P. Muggli *et al.*, Nature (London) **411**, 43 (2001).
[17] P. Muggli *et al.*, Phys. Rev. ST Accel. Beams **4**, 091301 (2001).
[18] J. Seeman *et al.*, Stanford Linear Accelerator Center Report No. SLAC-PUB-3945, 1986 (unpublished).
[19] P. Muggli *et al.*, IEEE Trans. Plasma Sci. **27**, 791 (1999).
[20] T. O. Raubenheimer, in *Advanced Accelerator Concepts, Eleventh Workshop*, edited by V. Yakimenko, AIP Conf. Proc. No. 737 (AIP, New York, 2004), p. 86.
[21] P. Muggli and J. S. T. Ng, in *Advanced Accelerator Concepts, Eleventh Workshop*, edited by V. Yakimenko, AIP Conf. Proc. No. 737 (AIP, New York, 2004), p. 206.
[22] P. Emma *et al.*, Stanford Linear Accelerator Center Report No. SLAC-PUB-8850, 2001 (unpublished).
[23] K. L. F. Bane *et al.*, Stanford Linear Accelerator Center Report No. SLAC-PUB-11035, 2005 (unpublished).
[24] K. L. F. Bane *et al.*, Stanford Linear Accelerator Center Report No. SLAC-PUB-5255, 1990 (unpublished); Stanford Linear Accelerator Center Report No. SLAC-PUB-7536, 1997 (unpublished); Stanford Linear Accelerator Center Report No. SLAC-PUB-8118, 1999 (unpublished).